



## High mass resolution time of flight mass spectrometer for measuring products in heterogeneous catalysis in highly sensitive microreactors.

Andersen, Thomas; Jensen, Robert; Christensen, M. K.; Pedersen, Thomas; Hansen, Ole; Chorkendorff, I

*Published in:*  
Review of Scientific Instruments

*Link to article, DOI:*  
[10.1063/1.4732815](https://doi.org/10.1063/1.4732815)

*Publication date:*  
2012

*Document Version*  
Publisher's PDF, also known as Version of record

[Link back to DTU Orbit](#)

*Citation (APA):*  
Andersen, T., Jensen, R., Christensen, M. K., Pedersen, T., Hansen, O., & Chorkendorff, I. (2012). High mass resolution time of flight mass spectrometer for measuring products in heterogeneous catalysis in highly sensitive microreactors. *Review of Scientific Instruments*, 83(7). <https://doi.org/10.1063/1.4732815>

---

### General rights

Copyright and moral rights for the publications made accessible in the public portal are retained by the authors and/or other copyright owners and it is a condition of accessing publications that users recognise and abide by the legal requirements associated with these rights.

- Users may download and print one copy of any publication from the public portal for the purpose of private study or research.
- You may not further distribute the material or use it for any profit-making activity or commercial gain
- You may freely distribute the URL identifying the publication in the public portal

If you believe that this document breaches copyright please contact us providing details, and we will remove access to the work immediately and investigate your claim.

## High mass resolution time of flight mass spectrometer for measuring products in heterogeneous catalysis in highly sensitive microreactors

T. Andersen, R. Jensen, M. K. Christensen, T. Pedersen, O. Hansen et al.

Citation: *Rev. Sci. Instrum.* **83**, 075105 (2012); doi: 10.1063/1.4732815

View online: <http://dx.doi.org/10.1063/1.4732815>

View Table of Contents: <http://rsi.aip.org/resource/1/RSINAK/v83/i7>

Published by the [American Institute of Physics](http://www.aip.org).

---

### Related Articles

Towards secondary ion mass spectrometry on the helium ion microscope: An experimental and simulation based feasibility study with He<sup>+</sup> and Ne<sup>+</sup> bombardment

*Appl. Phys. Lett.* **101**, 041601 (2012)

High-efficiency cross-beam magnetic electron-impact source for improved miniature Mattauch-Herzog mass spectrometer performance

*Rev. Sci. Instrum.* **83**, 064101 (2012)

Online and offline experimental techniques for polycyclic aromatic hydrocarbons recovery and measurement

*Rev. Sci. Instrum.* **83**, 034101 (2012)

Isotope fractionation in surface ionization ion source of alkaline-earth iodides

*Rev. Sci. Instrum.* **83**, 02B506 (2012)

Design of a compact electron cyclotron resonance ion source for medium charge state light ions

*Rev. Sci. Instrum.* **83**, 02A322 (2012)

---

### Additional information on *Rev. Sci. Instrum.*

Journal Homepage: <http://rsi.aip.org>

Journal Information: [http://rsi.aip.org/about/about\\_the\\_journal](http://rsi.aip.org/about/about_the_journal)

Top downloads: [http://rsi.aip.org/features/most\\_downloaded](http://rsi.aip.org/features/most_downloaded)

Information for Authors: <http://rsi.aip.org/authors>

## ADVERTISEMENT

The advertisement features a green and yellow abstract background with flowing lines. At the top, the 'AIP Advances' logo is displayed, with 'AIP' in blue and 'Advances' in green, accompanied by a series of orange dots. Below this, the text 'Special Topic Section: PHYSICS OF CANCER' is written in white, with 'PHYSICS OF CANCER' in a larger, bold font. At the bottom, the phrase 'Why cancer? Why physics?' is written in yellow, and a blue button with the text 'View Articles Now' is positioned on the right.

**AIP Advances**

Special Topic Section:  
**PHYSICS OF CANCER**

Why cancer? Why physics? [View Articles Now](#)

# High mass resolution time of flight mass spectrometer for measuring products in heterogeneous catalysis in highly sensitive microreactors

T. Andersen,<sup>1</sup> R. Jensen,<sup>1</sup> M. K. Christensen,<sup>1</sup> T. Pedersen,<sup>2</sup> O. Hansen,<sup>2</sup> and I. Chorkendorff<sup>1,a)</sup>

<sup>1</sup>*Department of Physics, Danish National Research Foundation's Center for Individual Nanoparticle Functionality (CINF), Technical University of Denmark, Building 312, DK-2800 Kgs. Lyngby, Denmark*

<sup>2</sup>*Department of Micro- and Nanotechnology, Technical University of Denmark, DTU Nanotech Building 345 East, DK-2800 Kgs. Lyngby, Denmark*

(Received 24 April 2012; accepted 17 June 2012; published online 10 July 2012)

We demonstrate a combined microreactor and time of flight system for testing and characterization of heterogeneous catalysts with high resolution mass spectrometry and high sensitivity. Catalyst testing is performed in silicon-based microreactors which have high sensitivity and fast thermal response. Gas analysis is performed with a time of flight mass spectrometer with a modified nude Bayard-Alpert ionization gauge as gas ionization source. The mass resolution of the time of flight mass spectrometer using the ion gauge as ionization source is estimated to  $m/\Delta m > 2500$ . The system design is superior to conventional batch and flow reactors with accompanying product detection by quadrupole mass spectrometry or gas chromatography not only due to the high sensitivity, fast temperature response, high mass resolution, and fast acquisition time of mass spectra but it also allows wide mass range (0–5000 amu in the current configuration). As a demonstration of the system performance we present data from ammonia oxidation on a Pt thin film showing resolved spectra of OH and NH<sub>3</sub>. © 2012 American Institute of Physics. [<http://dx.doi.org/10.1063/1.4732815>]

## I. INTRODUCTION

In heterogeneous catalysis optimization and development of analytic equipment is important both to minimize the cost of equipment but also to be able to experimentally study complicated systems. As a platform for testing heterogeneous catalysts, microfabricated reactors or microreactors have been found suitable due to both high surface-to-volume ratio, fast temperature response, and minimization of thermal and concentration gradients.<sup>1,2</sup> Such a platform has been developed to test and characterize model catalysts in our department.<sup>3</sup> However, a suitable reactor platform is only part of the task; reactant and product detection and characterization is essential to determine catalyst performance. Typically, quadrupole mass spectrometers (QMSs) are used in low pressure regimes to analyze gas composition while gas chromatographs (GCs) are used for high pressure measurements. The QMS, however, suffers from a low mass resolution ( $m/\Delta m \gtrsim m$  up to  $m \sim 200$ ) which makes analysis of complicated spectra difficult and cumbersome. Furthermore, QMSs are typically operated by logging a single (or a few) masses as a function of time to increase time resolution. This is at the expense of acquisition of full mass spectra during the experiment limiting operation by potentially losing interesting features in other masses not monitored. GCs have inherently low time resolution which make them unsuitable for fast time response measurements as in the case of microreactors and are in general difficult to use as mass spectrometers due to the difficult interpretation of measurements on complex mixtures. Furthermore, GCs only sample a very small part of the converted gas, making them unsuitable for small amounts of reactant and product gases

due to the low sensitivity. As an alternative to GCs or QMSs time of flight mass spectrometers (TOF-MS) offer both high mass resolution ( $m/\Delta m > 1000$ ), fast acquisition of full mass spectra ( $> 1$  Hz), and high sensitivity making them suitable for characterization of very small amounts of catalyst, i.e., model systems, and a mass range only limited by the detector. With a standard available microchannel plate (MCP) used as detector a mass range of 0–5000 amu can be obtained.

Typically, TOF-MS in heterogeneous catalysis is used as a surface analytic tool, i.e., TOF-SIMS.<sup>4–7</sup> Measurements of reactants and products on heterogeneous catalysts by TOF-MS have previously been performed<sup>8,9</sup> but, until now, to our knowledge, the testing of catalysts in a microreactor with subsequent gas analysis by a TOF-MS has not been demonstrated. Here we describe a microreactor and TOF-MS system which combines the high sensitivity of microreactors and the high mass resolution TOF-MSs for testing and characterizing of heterogeneous catalysts.

## II. SYSTEM DESIGN

The setup consists of three main components. The microreactor, where the catalyst under investigation is deposited, an ionization source which ionizes the gas from the microreactor and a TOF-MS used for gas analysis. In addition a QMS is connected to the capillary of the microreactor which enables direct comparison between the QMS and TOF-MS.

The catalyst under investigation is deposited in the microreactor reactor volume by e.g., evaporation,<sup>3</sup> drop casting,<sup>10</sup> or gas aggregation formed size-selected nanoparticles. The gas composition in the microreactor, reactor volume is ionized by the modified ion gauge and is subsequently

<sup>a)</sup>ibchork@fysik.dtu.dk.

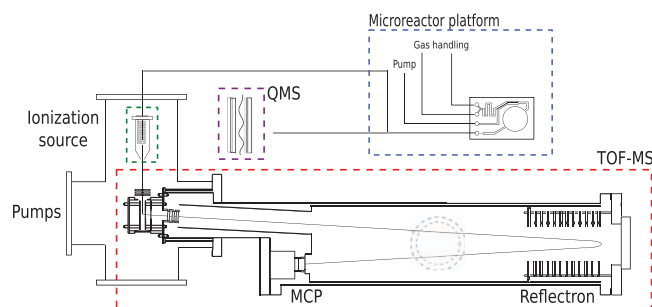


FIG. 1. Schematic of the total system (not to scale). The capillary outlet from the microreactor can be directed to either a QMS or the TOF-MS. For measurements by the TOF-MS, the gas is fed into a modified ion gauge which ionizes the gas. The ionized gas hereafter enters the TOF-MS through a series of Einzel lenses from where they are pushed into the flight tube by a repelling voltage,  $V_p$ . Ions are separated in the field free region and focused by the reflectron. The ions are subsequently detected by the MCP.

focused by the Einzel lenses into the source region. From the source region the ions are pushed into the flight tube by a repelling voltage pulse and is after mass separation in the flight tube detected by a MCP. A schematic of the entire setup is shown in Figure 1.

### A. The microreactor platform

Catalyst characterization and performance evaluation is performed in a microreactor.<sup>3</sup> The microreactors are silicon-based and measures  $20 \times 16$  mm. The reactor consists of two gas inlets, a gas outlet, a reactor volume, and a capillary used to restrict the gas flow from the reactor volume. The reactor volume is  $3 \mu\text{m}$  deep and 1 cm in diameter corresponding to a 236 nL volume. The diffusion length of the reactants and products gases in the microreactor reactor volume is almost an order of magnitude longer than the radius of the reactor volume ensuring full contact of the gas with the catalyst. This has been proven to hold by reproducible CO oxidation measurements on small Pt spots located at different points in the reactor volume. The two gas inlets are combined on the chip where the inlet gases mix by diffusion. The capillary is designed such that approximately  $3 \times 10^{14}$  molecules  $\text{s}^{-1}$  are probed from the reactor volume when operated at 1 bar. Any surplus of gas from the two inlets that does not enter the reactor volume is directed through an outlet to a turbo pump. The design ensures that all molecules or atoms entering the reactor volume, and hence exposed to the catalyst under investigation, are detected by mass spectrometry ensuring high sensitivity. This feature makes the microreactors especially well suited for characterization of model systems where small amounts of catalyst are typically used.

The microreactor is heated by joule heating of a 100 nm platinum strip (on top of a 3 nm Ti adhesion layer) evaporated through a shadow mask on the backside of the chip. The heating element is contacted by two pogo pins which are connected to a power supply. Two additional contacts are placed on the chip facilitating a four wire measurement of the resistance of the heating element. The heating strip can in this way be used as a resistance temperature detector (RTD) to determine the temperature of the chip. Currently, temperatures

from room temperature to  $\sim 450^\circ\text{C}$  can be reached due to apparatus limitations. The high temperature limit is expected to be  $\sim 600^\circ\text{C}$  where the pyrex lid used for sealing the reactor will melt.

### B. Gas handling for the microreactor

The two gas inlets on the microreactor chip are connected to a macroscopic gas handling system which is constructed entirely from UHV compatible elements to ensure extremely clean gas handling. A total of six gases with accompanying flow controllers are used to control the inlet gas flow to the microreactor. Currently, the system is configured in a  $4 + 2$  setup where four gases are connected to the first inlet and two gases connected to the secondary inlet. At the time of writing He, CO,  $\text{O}_2$ ,  $\text{CH}_4$ ,  $\text{NH}_3$ , and  $\text{H}_2$  are connected to the setup. All gases used on the setup are N6 quality gases, i.e., 99.9999 % purity. All valves and flow controllers are interfaced to a computer enabling remote control of the system and the ability to run experiments over several days without human intervention.

### C. Time of flight mass spectrometer

The time of flight chamber is pumped by a turbo pump and two ion pumps. A 120 l/s ion pump is used to pump the flight tube while a 400 l/s ion pump and a 450 l/s turbo pump are used to pump down the source region which is mounted on a 8 in. 4-way cross. Opposite to the source region of the TOF-MS the pumps are mounted while the two remaining flanges are occupied by the ionization gauge and a blanked flange (see Figure 1). While idling the pressure in the source region is  $\sim 1 \times 10^{-9}$  mbar and  $\sim 2 \times 10^{-9}$  mbar in the flight tube.

The time of flight equipment used for detection of gas molecules flown through the capillary of the microreactor is designed as an orthogonal mass spectrometer and is assembled from modules purchased from Jordan TOF Products, Inc.<sup>11</sup>

Ions enter the source region of the TOF-MS through a series of entry Einzel lenses used for focusing the beam hence minimizing divergence. In the source the beam is pushed into the flight tube by an initial repelling push voltage,  $V_p$ . The ions are hereafter further accelerated from ground potential to the liner potential,  $V_L$ . Using this setup the drift velocity of an ion starting exactly from the center of the acceleration region corresponds to an energy of  $Ze(V_L + V_p/2)$  where  $Ze$  is the charge of the ion. At the end of the flight tube a reflectron is installed. The reflectron is controlled by voltages  $V_{R1}$  and  $V_{R2}$ . The reflectron has two primary purposes: (1) The effective drift length is increased hence increasing the resolution of the TOF-MS. (2) The reflectron works as a focusing lens (cf. Figure 2) compensating for any initial velocity dispersion of the ions, i.e., ions with an initial higher velocity will have an increased flight length compared to slower ions. The MCP used for ion detection is placed in the focal point of the reflectron giving maximum compensation for initial velocity dispersion. According to the manufacturer a resolution  $m/\Delta m \gtrsim 4000$  of the TOF-MS has been shown.



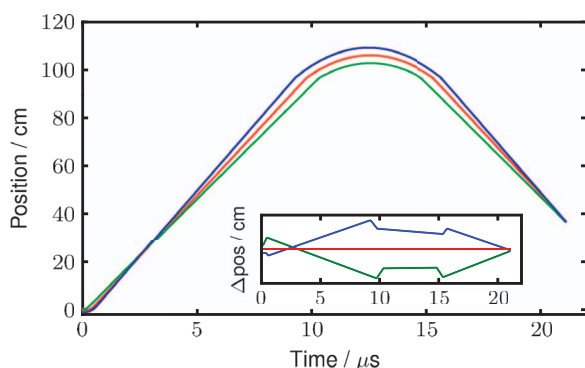


FIG. 2. Simulated trajectories of ions ( $m/q = 50$ ) with initial position variations in the source region illustrating the focusing effect of the reflectron. Red curve corresponds to ions with an initial position in the center of the source region while blue and green curves illustrate trajectories of ions with non-ideal initial positions displaced 6.3 mm towards and further away from the repelling plate, respectively. Inset shows the difference between displaced ions and the center positioned ion. The models does not include initial velocity dispersion of the ions.

The prize of the TOF including ionization gauge, 8 in. 4-way cross, control electronics, data acquisition hardware, and MCP detector is comparable to the prize of a high quality QMS with electronics making the TOF-MS a serious alternative to a QMS.

In Figure 3, an example spectrum of ammonia oxidation ( $\text{NH}_3:\text{O}_2$  4:3, 195 °C) is shown. Here the high resolution of the TOF-MS is demonstrated by resolving ammonia ( $\text{NH}_3$ ) and hydroxyl ( $\text{OH}$ ) which have a mass difference of 23 milli-amu.

## 1. Gas ionization

As ionization source of the gas flow from the microreactor capillary a modified nude UHV Bayard-Alpert ion gauge is used. A current of  $\sim 3$  A is run through the filament resulting in 10 mA emission current. The grid is biased  $\sim 40$  V neg-

ative compared to the filament to accelerate electrons emitted from the filament towards the grid. Contrary to standard operation of an ion gauge the collector in the center of the grid is short-circuited to the grid ensuring a homogeneous field distribution within the grid. To allow ionized ions to escape from the gauge the lid of the grid has been removed. Using this configuration approximately half of the ionized ions are expected to leave the ionization gauge.<sup>12</sup> The entire construction is placed in a flange with a small orifice which is differentially pumped by a turbo pump. Large amounts of gas can hence be dosed locally around the ion gauge while still maintaining a low pressure in the source region of the TOF-MS. The small orifice is essential in the setup to avoid high pressure in the acceleration region and drift tube of the TOF-MS which would cause an increase in dead counts on the MCP thus decreasing the signal-to-noise ratio of the recorded signal.

## 2. Data treatment

Raw data plotted with accompanying Gaussian fits are shown in Figure 4. Here the closely lying peaks from OH due to cracking of both residue water and water as reaction product and uncombusted  $\text{NH}_3$  is shown. The ability to separate these contributions substantially simplifies quantification of ammonia and allows for easier characterization of catalyst performance.

In Figure 5 raw data from water, hydrogen, and oxygen from three different regions are shown illustrating the dynamic range of the TOF-MS. At constant MCP voltage all the peaks are clearly visible although the ratio of the oxygen to water amplitude is  $\sim 400$ . In reality the dynamic range is limited mostly by the data acquisition hardware as well as the quality of the ion source. Even with the home-built ionization source and a 8-bit digitizer the dynamic range is, from Figure 5, estimated to be  $\sim 1000$  using an integration time of  $\sim 5$  s. The dynamic range of the TOF-MS is hence comparable to the dynamic range offered by a QMS at constant

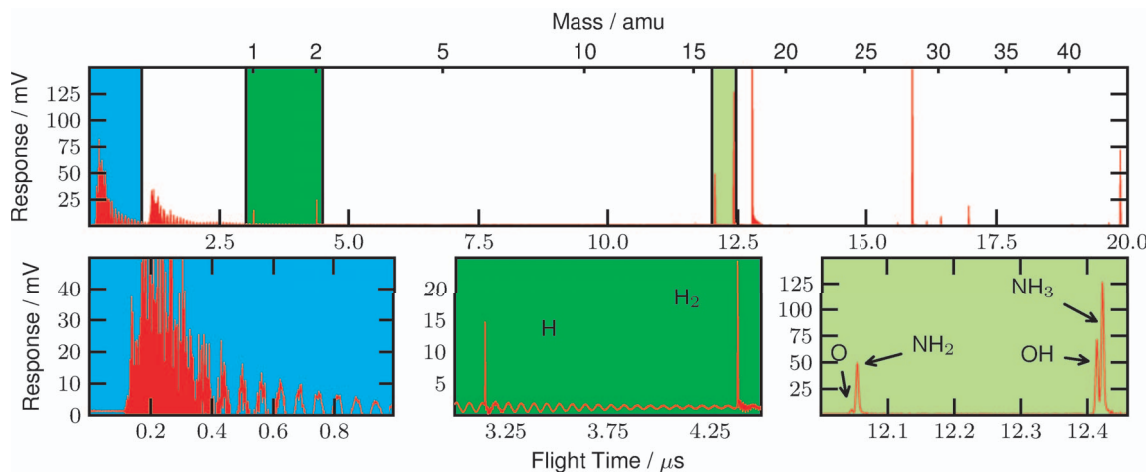


FIG. 3. Raw data acquired from the TOF-MS during  $\text{NH}_3$  oxidation by  $\text{O}_2$  ( $\text{NH}_3:\text{O}_2$  4:3, 195 °C). Subfigures show three different regions of the spectrum. From the first subfigure in the lower panel a delay between the acquisition trigger and the noise signal from the rise of the high voltage pulser of approximately 150 ns can be seen. This is due to delays in cables and the repeller pulser. In the center subfigure the extremely good separation between individual masses is shown. It is evident that 1 amu corresponds to  $\sim 1.4$   $\mu\text{s}$  difference in flight time in our system in the mass regime around 1 amu. In the last subfigure a zoom of the ammonia and hydroxyl peaks region shows separation between OH and  $\text{NH}_3$  as well as O and  $\text{NH}_2$  (23 milli-amu mass difference).

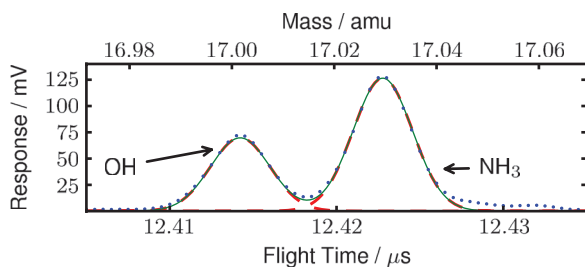


FIG. 4. Example of two Gaussian fits (dashed red lines) and the sum of the two fits (green solid line) to a double peak (blue dots) consisting of  $\text{NH}_3$  and  $\text{OH}$  both at  $\sim 17$  amu demonstrating the resolution of the TOF-MS. The entire graph section represents a mass difference of 100 milli-amu.

preamplifier range while covering a much larger mass range. The TOF-MS, however, acquires mass spectra (0–5000 amu) at high frequency ( $>1$  Hz) which is impossible with a QMS where only a few masses can be followed as a function of time to increase time resolution. The possibility of fast acquisition of complete mass spectra by the TOF-MS thus ensures that all masses are monitored simultaneously during the experiment. The problem of selecting appropriate masses for logging by the QMS is hence eliminated.

Since the TOF-MS only measures flight time and not the actual mass of the measured ions it is necessary to determine the relationship between flight time and actual mass. This can be done by calibration masses expressing known patterns in the mass spectrum. In this way masses can be reasonably well determined with subsequent fitting of these values to get an expression for the flight time as a function of mass. This approach is in some cases adequate but has the significant drawback that several peaks of well known masses must be present in the flight spectrum which is not always necessarily feasible. To determine the relationship between mass and flight time we have made a numeric model of the TOF-MS which calculates the flight time based only on the voltages for the pulser,  $V_p$ , liner,  $V_L$ , and reflectron,  $V_{R1}$  and  $V_{R2}$ , and thus provides a relationship of flight time to mass. Typically, the model is used together with the experimental determination of

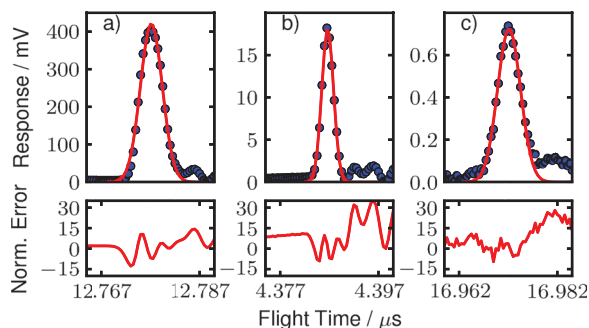


FIG. 5. Gaussian fits (red solid line) to three different mass to charge ratios (blue points) from the same mass spectrum. In panels (a), (b) and (c) the  $\text{H}_2\text{O}$  (peak area:  $2.35 \text{ mV} \cdot \mu\text{s}$ ),  $\text{H}_2$  (peak area:  $5.43 \times 10^{-2} \text{ mV} \cdot \mu\text{s}$ ) and  $\text{O}_2$  (peak area:  $4.24 \times 10^{-3} \text{ mV} \cdot \mu\text{s}$ ) signals are shown, respectively. As seen from the response a high dynamic range of the TOF-MS is demonstrated by good Gaussian fits to all peaks. The TOF-MS can hence be used to monitor both very small and very large signal masses. At the bottom panel the area normalized error for each fit shows that the relative fit error is independent of the total peak area.

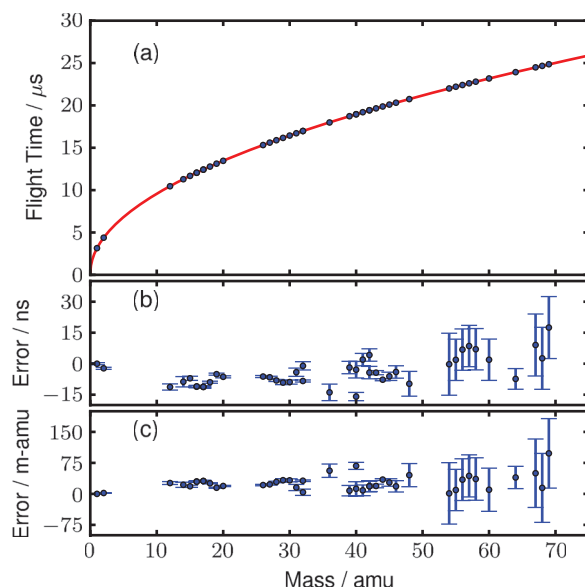
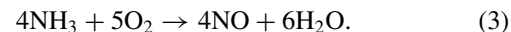
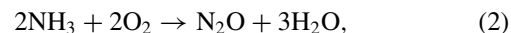


FIG. 6. Comparison of the simulated model (red curve, top panel) to actual measured experimental values (blue dots) of flight time as a function of mass. In the lower panels the difference between acquired experimental data and data calculated from the model in time and mass units are shown. Error bars represents only the uncertainty in the experimental data. As seen from the lower panels a deviation of  $\sim 10$  ns corresponding to  $\sim 50$  milli-amu at 70 amu is present.

a single mass since this will help fix the unknown delays originating from the measurement trigger, rise time of the high-voltage pulse at the repeller plate and cable delays. As seen in Figure 6 the performance of the model is good despite its simplicity giving a total error in flight time estimation of  $\sim 10$  ns corresponding to  $\sim 50$  milli-amu at 70 amu. The model is written in Python and can be acquired online.<sup>13</sup>

### III. OXIDATION OF AMMONIA

To demonstrate the system capability ammonia oxidation on a 1% geometrical coverage Pt thin film has been used as test reaction. The catalytic oxidation of ammonia can proceed along primarily three different routes.<sup>14</sup>



All of these systems are difficult to analyze both qualitatively and quantitatively due to the overlap of  $\text{NH}_3$ , which is a reactant, and  $\text{OH}$  originating from cracking of  $\text{H}_2\text{O}$ , which is a product from the combustion and is a part of the residue gas. Specifically, hydroxyls ( $\text{OH}$ ) from cracking of trace water in the system and the combustion reaction and the primary peak of ammonia ( $\text{NH}_3$ ) are both detected at  $m/q \simeq 17$ . Without adequate mass resolution it is not possible to separate the two contributions resulting in difficult analysis. Often a charge to mass ratio without cracking from both products and residual gas in the system is used to quantify the amount of ammonia

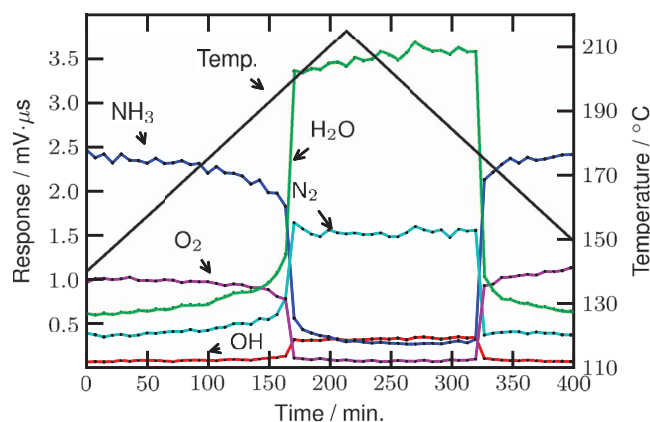


FIG. 7. Ammonia oxidation as a function of temperature on a 1% geometrical coverage Pt thin film. As the temperature is increased ammonia is oxidized to  $\text{H}_2\text{O}$  and  $\text{N}_2$ . Furthermore, the OH and  $\text{NH}_3$  signals are anticorrelated demonstrating the ability to resolve these two close lying masses as shown in Figure 4.

and water. In the case of ammonia,  $m/q = 15$  or  $m/q = 8.5$  is typically chosen since water does not contribute to these masses. However, both of these masses contains only a very small fraction of the main peak since it involves either the loss of two hydrogen atoms or a double charged ammonia ion which are both formed in processes with very low yields. The measurement of these masses have a very poor signal to noise ratio making measurements on ammonia very difficult with traditional mass spectrometry methods.

At the start of the experiment, the microreactor is equilibrated with  $\text{NH}_3$  and  $\text{O}_2$  in a 4:3 ratio corresponding to stoichiometry for this reaction. After equilibration the temperature is increased in steps of  $2.5^\circ\text{C}$  from  $150^\circ\text{C}$  to  $215^\circ\text{C}$ . The gas composition in the microreactor is continuously probed by the TOF-MS which is connected to the capillary of the microreactor. In Figure 7 the integrated  $\text{N}_2$ ,  $\text{NH}_3$ ,  $\text{H}_2\text{O}$ ,  $\text{O}_2$ , and OH peaks acquired from the raw TOF-MS spectrum as a function of temperature are shown. At each individual temperature step a mass scan is performed from triggering of the acceleration pulse up to  $25\ \mu\text{s}$  of flight time corresponding to 70 amu. As seen from Figure 7 the combustion of  $\text{NH}_3$  increases substantially at  $\sim 200^\circ\text{C}$  and drops again at  $\sim 175^\circ\text{C}$ . The combustion of ammonia to molecular nitrogen and water in this temperature range agrees well with literature.<sup>14,15</sup>

In Figure 7 an anticorrelation between OH and  $\text{NH}_3$  is seen. The inverse relation between these two masses can only be measured because these peaks are resolved in the mass spectrum. As expected a strong correlation between  $\text{H}_2\text{O}$  and OH is seen as a direct result of water cracking to hydroxyls. The data shown in Figure 7 hence demonstrates the usability of the combined microreactor and TOF-MS setup especially simplifying data analysis of complicated mass spectra while maintaining a high sensitivity from the microreactor platform.

#### IV. CONCLUSION

We have demonstrated a combined microreactor and TOF-MS system which can be employed to test and characterize model heterogeneous catalysts. An automated gas han-

dling system is used to flow gas over a catalyst in a microreactor volume from where gases can be probed. The reactor gas composition is directed through a flow restriction in the microreactor and subsequently analyzed by a TOF-MS combining high sensitivity and high mass resolution.

As a demonstration of the system performance ammonia oxidation on 1% geometrical coverage Pt thin film was performed. The ability to resolve OH and  $\text{NH}_3$  which is separated by 23 milli-amu was demonstrated. The resolution of reactants and products enables simple and straightforward quantification of the ammonia and water signals. This greatly simplifies the analysis compared to conventional QMSs used for gas analysis. The setup is furthermore superior to conventional QMSs where only a limited mass resolution at high masses can be obtained and can be applied to the study of small amounts of catalysts.

#### ACKNOWLEDGMENTS

This work was carried out as part of the Catalysis for Sustainable Energy initiative, which is funded by the Danish Ministry of Science, Technology and Innovation. The Center for Individual Nanoparticle Functionality is funded by the Danish National Research Foundation.

- <sup>1</sup>K. F. Jensen, "Microreaction engineering – is small better?" *Chem. Eng. Sci.* **56**(2), 293–303 (2001).
- <sup>2</sup>K. Jähnisch, V. Hessel, H. Löwe, and M. Baerns, "Chemistry in microstructured reactors," *Angew. Chem. Int. Ed.* **43**(4), 406–446 (2004).
- <sup>3</sup>T. R. Henriksen, J. L. Olsen, P. Vesborg, I. Chorkendorff, and O. Hansen, "Highly sensitive silicon microreactor for catalyst testing," *Rev. Sci. Instrum.* **80**(12), 124101 (2009).
- <sup>4</sup>A. Benninghoven, "Chemical-analysis of inorganic and organic-surfaces and thin-films by static time-of-flight secondary-ion mass-spectrometry (TOF-SIMS)," *Angew. Chem. Int. Ed.* **33**(10), 1023–1043 (1994).
- <sup>5</sup>F. De Smet, M. Devillers, C. Poleunis, and P. Bertrand, "Time-of-flight SIMS study of heterogeneous catalysts based on praseodymium and molybdenum oxides," *J. Chem. Soc., Faraday Trans.* **94**(7), 941–947 (1998).
- <sup>6</sup>J. Grams, J. Goralski, and T. Paryjczak, "High resolution surface imaging of Co/ZrO<sub>2</sub> catalyst by TOF-SIMS," *Surf. Sci.* **549**(1), L21–L26 (2004).
- <sup>7</sup>G. E. Johnson, M. Lysonski, and J. Laskin, "In situ reactivity and TOF-SIMS analysis of surfaces prepared by soft and reactive landing of mass-selected ions," *Anal. Chem.* **82**(13), 5718–5727 (2010).
- <sup>8</sup>E. J. Levy, E. D. Miller, and W. S. Beggs, "Application of time of flight mass spectrometry and gas chromatography to reaction studies," *Anal. Chem.* **35**(8), 946–949 (1963).
- <sup>9</sup>K. Okumura, Y. Sakamoto, T. Kayama, Y. Kizaki, H. Shinjoh, and T. Motohiro, "Quantitative analysis of transient surface reactions on planar catalyst with time-resolved time-of-flight mass spectrometry," *Rev. Sci. Instrum.* **78**(10), 104102 (2007).
- <sup>10</sup>P. C. K. Vesborg, J. L. Olsen, T. R. Henriksen, I. Chorkendorff, and O. Hansen, "Gas-phase photocatalysis in mu-reactors," *Chem. Eng. J.* **160**(2), 738–741 (2010).
- <sup>11</sup>See <http://www.rmjordan.com/OrthogoTOF/orthogotof.html> for specific details from the manufacturer.
- <sup>12</sup>W. B. Nottingham, *Vacuum Symposium Transactions* (Committee on Vacuum Techniques, Boston, 1955).
- <sup>13</sup>See <https://github.com/robertjensen/FlightTime> to download the Python source code to perform the simulation.
- <sup>14</sup>R. Imbihl, A. Scheibe, Y. F. Zeng, S. Gunther, R. Kraehnert, V. A. Kondratenko, M. Baerns, W. K. Offermans, A. P. J. Jansen, and R. A. van Santen, "Catalytic ammonia oxidation on platinum: mechanism and catalyst restructuring at high and low pressure," *Phys. Chem. Chem. Phys.* **9**(27), 3522–3540 (2007).
- <sup>15</sup>Y. F. Zeng and R. Imbihl, "Structure sensitivity of ammonia oxidation over platinum," *J. Catal.* **261**(2), 129–136 (2009).